

Radiation Driven Implosion and Triggered Star Formation

T. G. Bisbas¹, A. P. Whitworth², R. Wünsch¹, D. A. Hubber³,
and S. Walch²

¹Astronomical Institute, Academy of Sciences of the Czech Republic, Boční II 1401, 141 31 Prague, Czech Republic. Email: t.bisbas@astro.cf.ac.uk

²School of Physics and Astronomy, Cardiff University, Queens Buildings, The Parade, Cardiff, CF24 3AA, United Kingdom

³Department of Physics and Astronomy, University of Sheffield, Hicks Building, Hounsfield Road, Sheffield S3 7RH, United Kingdom

Abstract. We present simulations of stable isothermal clouds exposed to ionizing radiation from a discrete external source, and identify the conditions that lead to Radiatively Driven Implosion and Star Formation. We use the Smoothed Particle Hydrodynamics code SEREN (Hubber *et al.* 2010) and the HEALPix-based photoionization algorithm described in Bisbas *et al.* (2009). We find that the incident ionizing flux is the critical parameter determining the evolution; high fluxes disperse the cloud, whereas low fluxes trigger star formation. We find a clear connection between the intensity of the incident flux and the parameters of star formation.

Keywords. hydrodynamics, methods: numerical, stars: formation, (ISM:) HII regions

1. Introduction

When an expanding HII region overruns a pre-existing cloud, it compresses it by driving an ionization front and a shock wave into it (Sandford *et al.* 1982; Bertoldi 1989; Lefloch & Lazareff 1994). The inner parts may become gravitationally unstable and collapse to form new stars. This mechanism is known as Radiation Driven Implosion (RDI). Observations (Lefloch & Lazareff 1995; Lefloch *et al.* 1997; Sugitani *et al.* 1999, 2000; Ikeda *et al.* 2008; Morgan *et al.* 2008; Chahuan *et al.* 2009) strongly support a connection between the RDI mechanism and the formation of Young Stellar Objects (YSO). Simulations of the interaction of ultraviolet ionizing radiation with self-gravitating clouds have been presented by various authors (Kessel-Deynet & Burkert 2003; Esquivel & Raga 2007; Gritschneider *et al.* 2009; Miao *et al.* 2009). However, no model can explain *where* star formation takes place (in the core or at the periphery) or *when* (during the maximum compression phase or earlier – Deharveng *et al.* 2005). The aim of this work is to answer questions of whether the ionizing radiation incident upon stable clouds is able to trigger the formation of new stars or not, and how the process and the properties of this star formation are connected with the intensity of the incident flux. In Section 2 we give a brief description of the numerical treatment and the initial conditions we use. In Section 3 we discuss the results of our simulations. We summarize in Section 4.

2. Numerical Treatment and Initial Conditions

We use the Smoothed Particle Hydrodynamics (SPH) code SEREN[†], fully described in Hubber *et al.* (2010), with an ionization routine (Bisbas *et al.* 2009) based on the

[†] <http://www.astro.group.shef.ac.uk/seren>

HEALPix[‡] sphere tessellation code (Górski *et al.* 2005). We use a barotropic equation of state (i.e. Bonnell 1994) to set the temperature of the neutral gas as $T_N(\rho) = T_{\text{ISO}} \left\{ 1 + (\rho/\rho_{\text{CRIT}})^{\gamma-1} \right\}$, where $T_{\text{ISO}} = 10 \text{ K}$, $\rho_{\text{CRIT}} = 10^{-13} \text{ g cm}^{-3}$ and $\gamma = 5/3$ is the ratio of specific heats. The temperature of the ionized gas is set to $T_i = 10^4 \text{ K}$, except in the transition zone between the two extremes, where it changes smoothly from T_i to T_N (see Bisbas *et al.* 2009). We include sink particles (Bate *et al.* 1995) with radii $R_{\text{SINK}} = 2.5 \text{ AU}$ created if $\rho > \rho_{\text{SINK}} = 10^{-11} \text{ g cm}^{-3}$.

Our clouds are stable Bonnor-Ebert spheres (hereafter ‘BES’) with dimensionless cut-off radii $\xi_B = 4, 5, 6$ (see Bonnor 1956 for its definition) and with masses $M = 2, 5, 10 M_\odot$. The particle resolution we use is 5×10^4 SPH particles per solar mass (cf. Hubber *et al.* 2006). We use a single source emitting Lyman- α photons. We place the BESs at distance $D = 10R$ from the ionizing source, where R is the radius of the cloud (in pc), in order to keep constant the divergence of the incident flux and as parallel as possible. We run simulations with a wide range of emission rates $\dot{N}_{\text{Ly}\alpha} = 10^x \text{ s}^{-1}$, where $x = 48, 48.5, \dots, 52$.

3. Results

In Fig.1a we present a semi-logarithmic diagram where we correlate the intensity of the incident ionizing flux with the initial mass of each BES. The lines define subsets of parameter space where models either show star formation (left) or not (right), with accuracy 0.25 dex. It can be seen that as the mass of the BES decreases (and as a result ξ_B increases) the clouds appear to dissolve in higher fluxes. This is because for a given ξ_B , the density ρ_c at the centre of each BES increases with decreasing M .

We also find that the Strömgen radius at the end of the R -type expansion determines whether stars are formed or not; if the ionization front has not overrun the central core of the BES, then the incident flux will trigger star formation during the D -type expansion of the HII region. In the opposite case there is not enough material to undergo gravitational collapse and form stars.

The time, t_{SINK} , between the beginning of the D -type expansion and the first sink creation (beginning of star formation) increases with decreasing ionizing flux. This finding is in agreement with simulations of the RDI performed by Gritschneider *et al.* (2009). Figure 1b is a logarithmic diagram where we plot the values of t_{SINK} versus the incident flux Φ_D . Remarkably, it can be seen that t_{SINK} does not depend on ξ_B . Results from our simulations can be described with a power law of the form $t_{\text{SINK}} = 80 \times \Phi_D^{-0.3}$ (t_{SINK} in Myr, Φ_D in $\text{cm}^{-2}\text{s}^{-1}$).

Figure 2 shows column density plots of a BES with $M = 10M_\odot$ and with $\xi_B = 6$ at t_{SINK} for different fluxes. A common feature in all our simulations is that stars form close to the symmetry axis joining the centre of the cloud to the exciting star. This is probably a consequence of the initial spherical symmetry of the cloud and it is in an agreement with observations by Sugitani *et al.* (1999). The distance d_t between the first sink particle and the ionization front is a function of the ionizing flux and the BES parameters (see Fig.1c where we plot $d_t/2R$ for all BESs with $\xi_B = 6$). We find that for low fluxes stars tend to form away from the periphery, whereas for high fluxes stars tend to form at the periphery of the cloud. Similar results are found also with $\xi_B = 4$ and $\xi_B = 5$.

Figure 2 shows that the lateral compression, w_d , of the BESs at the beginning of star formation is connected to the intensity of the incident flux. We see that for low fluxes, w_d is quite high and the cloud has a U-shape structure, whereas for high fluxes w_d is small and the cloud has a V-shape structure. In Fig.1d we plot $w_d/2R$ for all BESs with $\xi_B = 6$

[‡] <http://healpix.jpl.nasa.gov>

and we find that stars tend to form during maximum compression once the incident flux is increased. Similar results are found also for the rest of the clumps.

4. Conclusions

We present simulations of RDI in stable clouds represented by BESs. We performed 75 simulations with clouds of different masses, different dimensionless radii, and with a wide range of incident fluxes. In general we find a connection between the incident ionizing flux and whether the cloud is induced to form stars or not by the flux. Our results only apply to clouds which have similar density structures.

We introduce a semi-logarithmic diagram (flux-mass diagram) where we correlate the intensity of the incident flux and the initial mass of each BES, and we define zones of Star Formation and no-Star Formation. We find that if the Strömgen radius has not overrun the central core of the BES by the end of the R -type expansion, the ionizing radiation will trigger star formation. The time when star formation occurs increases with decreasing flux, and does not depend on ξ_B . A power-law of the form $t_{\text{SINK}} = 80 \times \Phi_D^{-0.3}$ fits very well with the results of our models. Finally, as the incident flux increases, stars tend to form closer to the periphery of the cloud and during its maximum compression phase.

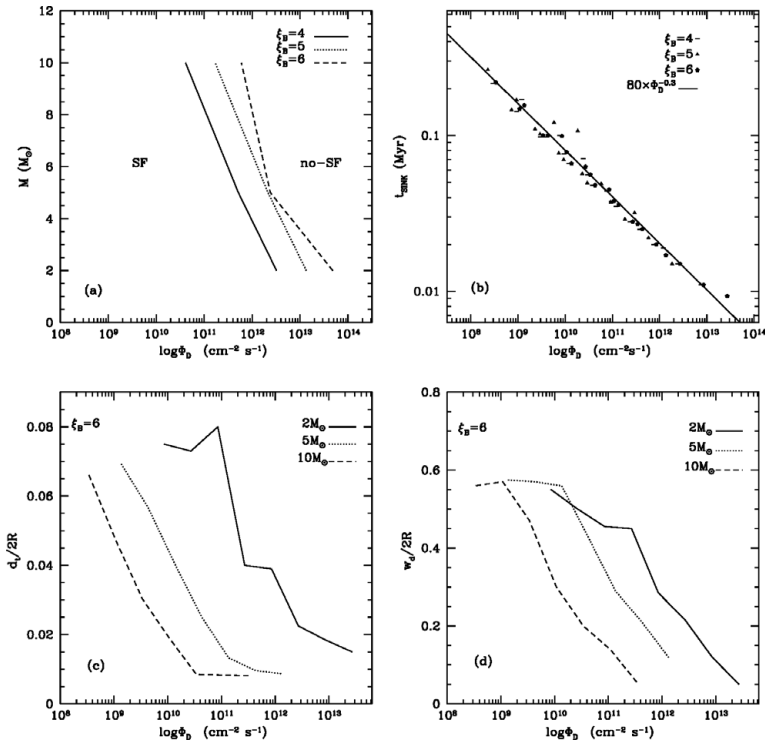


Figure 1. (a) The flux-mass semi-logarithmic diagram where we define areas where stars are formed (SF) and areas where stars are not formed (no-SF) depending on the dimensionless radius ξ_B of a BES. (b) Logarithmic diagram of the incident flux versus t_{SINK} . The power law we propose (solid line) fits very well with our simulations (t_{SINK} is in Myr and Φ_D is in $\text{cm}^{-2} \text{s}^{-1}$). (c) Star formation occurs at the periphery with increasing flux. (d) Star formation occurs during maximum compression with increasing flux.

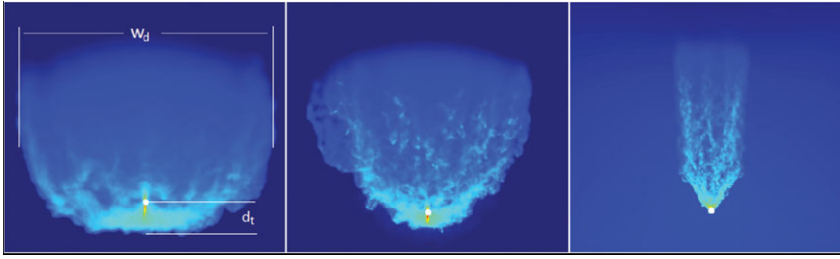


Figure 2. Column density plots of a BES with $M = 10 M_{\odot}$ and $\xi_B = 6$ at t_{SINK} when it is exposed to three different intensities of flux (flux increases from left to right). The white dots are sink particles. In the left plot we draw the values of d_t and w_d .

Acknowledgments: TGB and RW acknowledge support from the project LC06014-Centre for Theoretical Astrophysics of the Ministry of Education, Youth and Sports of the Czech Republic. APW and SW gratefully acknowledge the support of the Marie Curie Research Training Network CONSTELLATION (Ref. MRTN-CT-2006-035890). DAH is funded by a Leverhulme Trust Research Project Grand (F/00 118/BJ). The computations in this work were carried out on Merlin Supercomputer of Cardiff University. The column density plots were made using the SPLASH visualization code (Price 2007). The authors acknowledge the anonymous referee for the useful comments.

References

- Barnes, J. & Hut, P. 1986, *Nature*, 324, 446
 Bate, M. R., Bonnell, I. A., & Price, N. M. 1995, *MNRAS*, 277, 362
 Bertoldi, F. 1989, *ApJ*, 346, 735
 Bisbas, T. G., Wünsch, R., Whitworth, A. P., & Hubber, D. A. 2009, *A&A*, 497, 649
 Bonnell, I. A. 1994, *MNRAS*, 269, 837
 Bonnor, W. B. 1956, *MNRAS*, 116, 351
 Chauhan, N., Pandey, A. K., Ogura, K., Ojha, D. K., Bhatt, B. C., Ghosh, S. K., & Rawat, P. S. 2009, *MNRAS*, 396, 964
 Esquivel, A. & Raga, A. C. 2007, *MNRAS*, 377, 383
 Deharveng, L., Zavagno, A., & Caplan, J. 2005, *A&A*, 433, 565
 Górski, K. M., Hivon, E., Banday, A. J., Wandelt, B. D., Hansen, F. K., Reinecke, M., & Bartelmann, M. 2005, *ApJ*, 622, 759
 Gritschneider, M., Naab, T., Burkert, A., Walch, S., Heitsch, F., & Wetzstein, M. 2009, *MNRAS*, 393, 21
 Hubber, D. A., Batty, C. P., McLeod, A., & Whitworth, A. P., 2010, *A&A*, submitted
 Hubber, D. A., Goodwin, S. P., & Whitworth, A. P. 2006, *A&A*, 450, 881
 Ikeda, H., *et al.* 2008, *AJ*, 135, 2323
 Kessel-Deynet, O. & Burkert, A. 2003, *MNRAS*, 338, 545
 Lefloch, B. & Lazareff, B. 1994, *A&A*, 289, 559
 Lefloch, B. & Lazareff, B. 1995, *A&A*, 301, 522
 Lefloch, B., Lazareff, B., & Castets, A. 1997, *A&A*, 324, 249
 Miao, J., White, G. J., Thompson, M. A., & Nelson, R. P. 2009, *ApJ*, 692, 382
 Monaghan, J. J. 1992, *ARAA*, 30, 543
 Morgan, L. K., Thompson, M. A., Urquhart, J. S., & White, G. J. 2008, *A&A*, 477, 557
 Price, D. J. 2007, Publications of the Astronomical Society of Australia, 24, 159
 Sandford, M. T., II, Whitaker, R. W., & Klein, R. I. 1982, *ApJ*, 260, 183
 Sugitani, K., Tamura, M., & Ogura, K. 1999, Star Formation 1999, Proceedings of Star Formation 1999, held in Nagoya, Japan, June 21 - 25, 1999, Editor: T. Nakamoto, Nobeyama Radio Observatory, p. 358-364, 358
 Sugitani, K., Matsuo, H., Nakano, M., Tamura, M., & Ogura, K. 2000, *AJ*, 119, 323